Available online at www.sciencedirect.com
ScienceDirect
International Journal of Thermal Sciences 47 (2008) 1316–1331
International Journal of Thermal Sciences
www.elsevier.com/locate/ijts

Numerical analysis of natural convection in an inclined trapezoidal enclosure filled with a porous medium

Yasin Varol [a], Hakan F. Oztop [b], Ioan Pop [c,*]

[a] *Department of Mechanical Education, Firat University, 23119 Elazig, Turkey*
[b] *Department of Mechanical Engineering, Firat University, 23119 Elazig, Turkey*
[c] *Faculty of Mathematics, University of Cluj, CP 253, R-3400 Cluj, Romania*

Received 19 April 2007; received in revised form 26 October 2007; accepted 26 October 2007

Available online 20 February 2008

Abstract

A theoretical study of buoyancy-driven flow and heat transfer in an inclined trapezoidal enclosure filled with a fluid-saturated porous medium heated and cooled from inclined walls has been performed in this paper. The governing non-dimensional equations were solved numerically using a finite-difference method. The effective governing parameters are: the orientation or inclination angle of the trapezoidal enclosure ϕ, which varies between 0° and 180°, the Rayleigh number Ra, which varies between 100 and 1000, the side wall inclination angle θ_s and the aspect ratio A. The side wall inclination parameter θ_s is chosen as 67°, 72° and 81° and the calculations are tested for two different values of $A = 0.5$ and 1.0. Streamlines, isotherms, Nusselt number and flow strength are presented for these values of the governing parameters. The obtained results show that inclination angle ϕ is more influential on heat transfer and flow strength than that of the side wall inclination angle θ_s. It is also found that a Bénard regime occurs around $\phi = 90°$, which depends on the inclination of the side wall, Rayleigh number and aspect ratio.

Keywords: Trapezoidal enclosure; Porous medium; Natural convection; Numerical solution

1. Introduction

Applications of porous media include utilization of geothermal energy, design of packed bed reactors, energy storage systems, solar collectors, heat exchangers, etc. These are some of applications and the most of studies in porous media have been recently excellently reviewed by Ingham and Pop [1], Nield and Bejan [2], Ingham et al. [3], Bejan et al. [4] and Vafai [5]. Also, a great number of published studies are related with the analysis of natural convection in square/rectangular enclosures, particularly, with differentially heated vertical walls via isothermal heaters and adiabatic horizontal walls. Some important numerical results can be found in the studies by Walker and Homsy [6], Bejan [7], Prasad and Kulacki [8], Beckermann et al. [9], Gross et al. [10], Lai and Kulacki [11], Goyeau et al. [12], Manole and Lage [13], Choi et al. [14], Mamou et al. [15] and Saeid and Pop [16]. Some studies have also been performed to investigate the effect of inclination on natural convection in inclined square/rectangular enclosures filled with porous media or viscous (non-porous) fluids [17–25].

However, the shape of cavities can be also non-rectangular in practical engineering applications such as solar collectors or heat exchangers with different shaped duct constructions. The study of convective flow in these kind of geometries are more difficult than that of square or rectangular enclosures due to presence of sloping walls. Flow and heat transfer in triangular [26–30], parallelogram [31] and trapezoidal enclosures [32–39] is mostly analyzed in the literature. The natural convection in an inclined trapezoidal enclosure at different inclination angles filled with a viscous fluid has been studied by Lee [34]. He made a numerical study for different values of the Prandtl number using body-fitted coordinate systems. It was shown that heat transfer in such an enclosure with two symmetrical, inclined sidewalls of moderate aspect ratios, is a strong function of the orientation angle of the enclosure for $Ra > 10^4$ and $Pr > 0.1$, where Pr is the Prandtl number. Kumar

* Corresponding author. Tel.: +40 264 594315; fax: +40 264 591906.
E-mail address: pop.ioan@yahoo.co.uk (I. Pop).

1290-0729/$ – see front matter
doi:10.1016/j.ijthermalsci.2007.10.018

Nomenclature

A	dimensionless aspect ratio ($A = H/L$)		
g	gravitational acceleration	m s^{-2}	
Gr	Grashof number		
H	height of the enclosure	m	
K	permeability	m^2	
L	length of the enclosure	m	
Nu	Nusselt number		
Ra	Rayleigh number for a porous medium		
T	fluid temperature	K	
u, v	velocity components along x- and y-axes	m s^{-1}	
x, y	dimensional coordinates along the horizontal and vertical walls of the enclosure, respectively	m	
X, Y	dimensionless coordinates		

Greek symbols

α_m	effective thermal diffusivity of the porous medium	m^2 s^{-1}
β	thermal expansion coefficient	K^{-1}
ϕ	inclination angle	
θ	dimensionless temperature	
θ_s	side wall inclination angle	
υ	kinematic viscosity	m^2 s^{-1}
ψ	dimensional stream function	m^2 s^{-1}
Ψ	dimensionless stream function	

Subscripts

C	cold
H	hot

and Kumar [32] used parallel computation technique to analyze the natural convection in a trapezoidal enclosure filled with a porous medium. In their case, the short bottom and long top walls are taken as adiabatic, while differentially heated sloping walls. It was shown that the flow and heat transfer distribution inside the enclosure is affected by the inclination of the side wall of the enclosure. Baytas and Pop [33] solved the Darcy and energy equations in cylindrical coordinates to analyze natural convection in a trapezoidal enclosure filled with a porous medium. They observed that up to Rayleigh number $Ra = 100$, a conduction-dominated regime prevails, and afterwards a two-cellular convective flow regime takes place at the tilt angle 165°.

The above literature survey clearly shows that the effects of inclination angle on natural convection in trapezoidal enclosures have not been studied yet. The principal aim of this paper is, therefore, to analyze the natural convection in an inclined two-dimensional trapezoidal enclosure filled with a fluid-saturated porous medium. The governing non-dimensional equations are solved numerically using a finite-difference method. The resulting local and mean Nusselt numbers and streamlines and isotherms are determined as a function of the Rayleigh number, inclination or orientation angle and inclination angle of the side wall of the trapezoidal enclosure.

2. Equations and numerical solution

The general schematic configuration is a two-dimensional trapezoid enclosure filled with a porous medium as shown in Fig. 1(a) along with the coordinates and boundary conditions. The grid distribution for numerical solution is shown in Fig. 1(b). Regular distributed grids are used in this study. The sloping walls of the trapezoidal enclosure are heated and cooled at constant temperatures T_H and T_C, respectively, where $T_H > T_C$. The horizontal walls are kept as adiabatic. With the change of aspect ratio A ($= H/L$), the distance between nodes in vertical direction (Δy) is automatically changed. The governing equations for the steady, two-dimensional, incompressible flow with Darcy–Boussinesq approximation and constant fluid properties can be written in non-dimensional form as follows:

$$\frac{\partial^2\Psi}{\partial X^2} + \frac{\partial^2\Psi}{\partial Y^2} = Ra\left(\cos\phi\frac{\partial\theta}{\partial X} - \sin\phi\frac{\partial\theta}{\partial Y}\right) \tag{1}$$

$$\left(\frac{\partial\Psi}{\partial Y}\frac{\partial\theta}{\partial X} - \frac{\partial\Psi}{\partial X}\frac{\partial\theta}{\partial Y}\right) = \frac{\partial^2\theta}{\partial X^2} + \frac{\partial^2\theta}{\partial Y^2} \tag{2}$$

where the dimensionless variables are defined as

$$X = \frac{x}{L}, \qquad Y = \frac{y}{L}, \qquad \Psi = \frac{\psi}{\alpha_m}$$
$$(U, V) = \frac{(u, v)H}{\alpha_m}, \qquad \theta = \frac{T - T_C}{T_H - T_C} \tag{3}$$

Here x and y are the Cartesian coordinates along the horizontal and vertical walls of the enclosure, respectively, u and v are the velocity components along the x- and y-directions, θ is the non-dimensional fluid temperature, Ψ is the non-dimensional stream function, which is defined as

$$U = \frac{\partial\Psi}{\partial Y}, \qquad V = -\frac{\partial\Psi}{\partial X} \tag{4}$$

and the other quantities are defined in the nomenclature. The Rayleigh number Ra for the porous medium is defined as

$$Ra = \frac{g\beta K(T_H - T_C)L}{\upsilon\alpha_m} \tag{5}$$

The boundary conditions of Eqs. (1) and (2), as shown in Fig. 1(a), are $\Psi = 0$ for all solid boundaries, $\theta = 1$ on the hot wall, $\theta = 0$ on the cold wall and $\frac{\partial\theta}{\partial n} = 0$ on the adiabatic walls, where n denotes the direction normal to the inclined wall of the enclosure.

Besides the streamlines and isotherms, the physical quantities of interest in this problem are also the local, Nu_y, and the mean, Nu_m, Nusselt numbers from the heated wall, which are given by

$$Nu_y = \left(-\frac{\partial\theta}{\partial X}\right)_{X=0}, \qquad Nu_m = \frac{1}{A}\int_0^A Nu_y\,\mathrm{d}Y \tag{6}$$

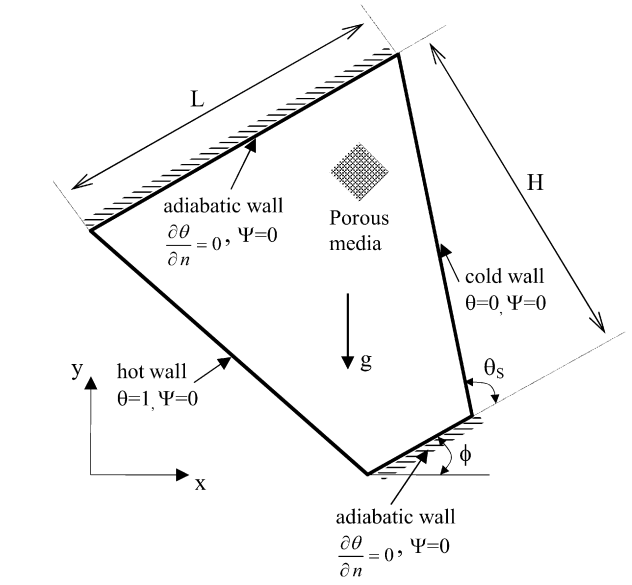

a)

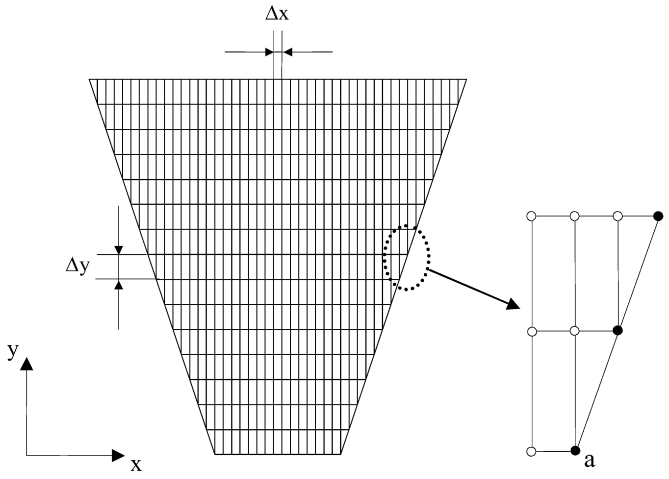

b)

Fig. 1. (a) Physical model, (b) grid distribution.

2.1. Numerical technique

Central finite-difference method has been used to discretize the governing non-dimensional equations, Eqs. (1) and (2). The solution of the linear algebraic equations has been performed using Successive Under Relaxation (SUR) method. The solution domain consists of grid points at which equations are applied. Table 1 shows optimal grid dimensions for different side wall inclination angle θ_s. To obtain grid-independent solution, different grid dimensions were obtained for each θ_s and chosen grid dimensions were given inside dashed ellipsoid. Distance between nodes are denoted by Δx and Δy in the x- and y-directions, respectively. As it is shown in Table 1, the 181×76 grid dimensions have been chosen for 67°, 181×61 for 72°, and 181×31 for 81°, respectively. The inclined wall is approximated by staircase-like zigzag lines. The bold circles shown in Fig. 1(b) are boundary nodes and they have Dirichlet boundary conditions. Values of internal nodes are calculated using boundary values via a central finite-difference method and the iteration process is terminated when the following condition is satisfied

$$\sum_{i,j} |\Phi_{i,j}^{m} - \Phi_{i,j}^{m-1}| \Big/ \sum_{i,j} |\Phi_{i,j}^{m}| \leqslant 10^{-5} \tag{7}$$

where Φ stands for either θ or Ψ, and m denotes the iteration step. Due to lack of suitable results in the literature pertaining to the present configuration, the present results have been validated against the existing results for a square cavity filled with a porous medium. Thus, the comparison of the present results for the mean Nusselt number Nu_m, as defined by Eq. (6), with those from the open literature has been made for a value of $Ra = 1000$. The results are given in Table 2. It is worth mentioning that Baytas and Pop [31] and Saeid and Pop [16] used the same method as in the present study. However, Goyeau et al. [12] used Darcy–Brinkman method to study their problem. We can see that the present values of Nu_m are in good agreement with those obtained by various authors. Maximum difference of 5% is found for Nu_m at $Ra = 1000$. For a rectangular enclosure, contours of streamlines and isotherms are almost the same as the ones given in the literature. However, they are not presented here to save space. A second test was performed

Table 1
Optimal grid dimensions for different inclination angle of the sidewall at $\phi = 0°$ and $Ra = 1000$

Inclination angle of the sidewall (θ_s)	Grid dimension (X by Y)	Mean Nusselt number (Nu_m)
67°	101×36	10.43
	141×56	10.95
	181×76	9.23
	221×96	9.65
72°	101×21	9.17
	141×41	9.75
	181×61	8.96
	221×81	8.81
81°	161×21	8.93
	181×31	8.42
	201×41	7.95
	221×51	8.25

Table 2
Comparison of the mean Nusselt number Nu_m for a square porous cavity with some results from the open literature at $Ra = 1000$

References	Nu_m
Bejan [7]	15.800
Gross et al. [10]	13.448
Goyeau et al. [12]	13.470
Manole and Lage [13]	13.637
Saeid and Pop [16]	13.726
Baytas and Pop [31]	14.060
Present result	13.564

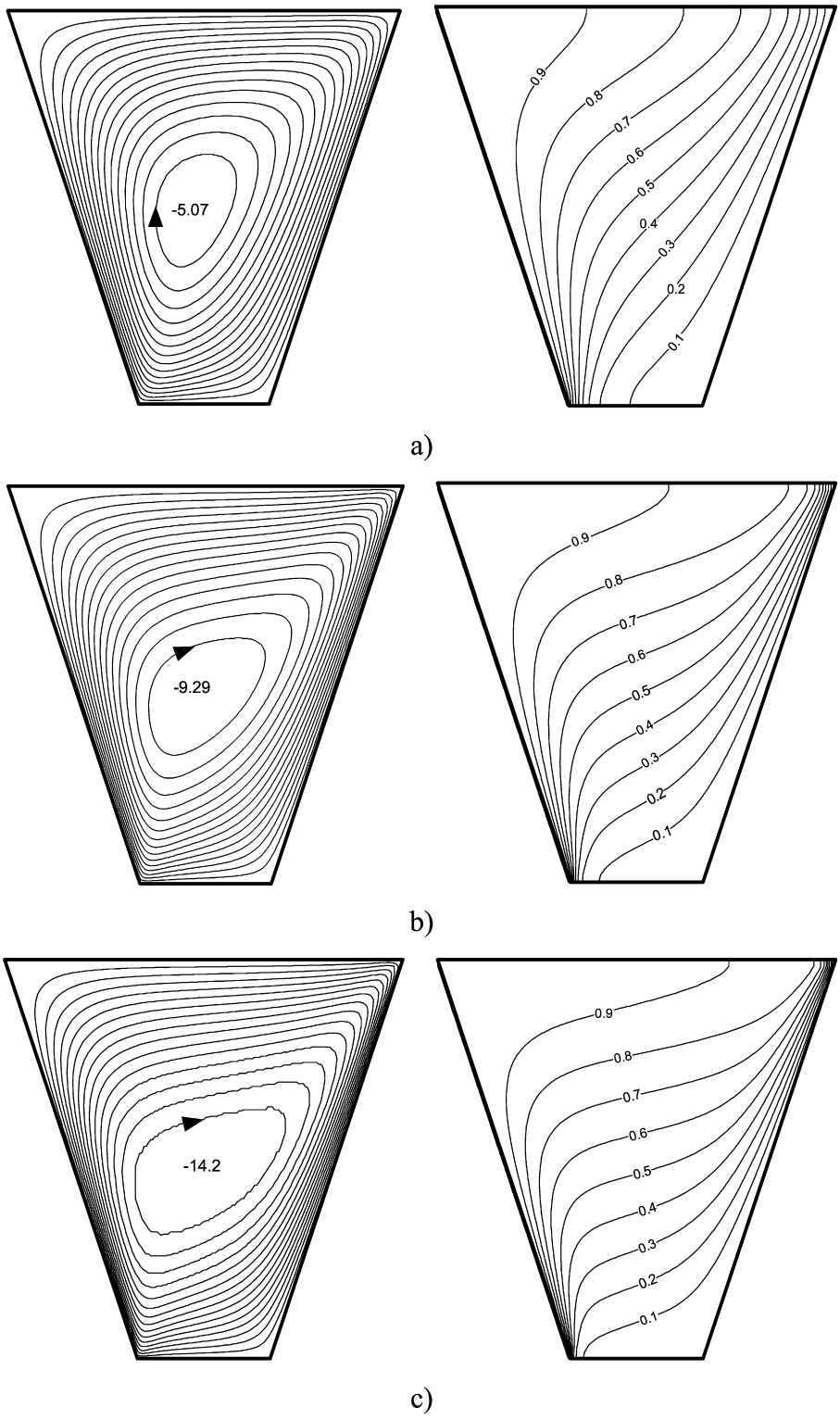

Fig. 2. Streamlines (on the left) and isotherms (on the right) for $A = 1.0$, $\theta_s = 72°$, $\phi = 0°$; (a) $Ra = 100$, (b) $Ra = 250$, (c) $Ra = 500$.

to show validation of the code with literature as given in Table 3. In this case, the results are compared with those reported by Baytas and Pop [31] which refers to a parallelogram cavity filled with a fluid saturated porous medium. It is seen that the present results show good agreement with those of Baytas and Pop [31].

Table 3
Comparison of the mean Nusselt number Nu_m for $Ra = 100$

θ_s	15°	30°	45°
Nu_m (Ref. [31])	2.95	2.62	2.23
Nu_m (present)	2.872	2.585	2.217

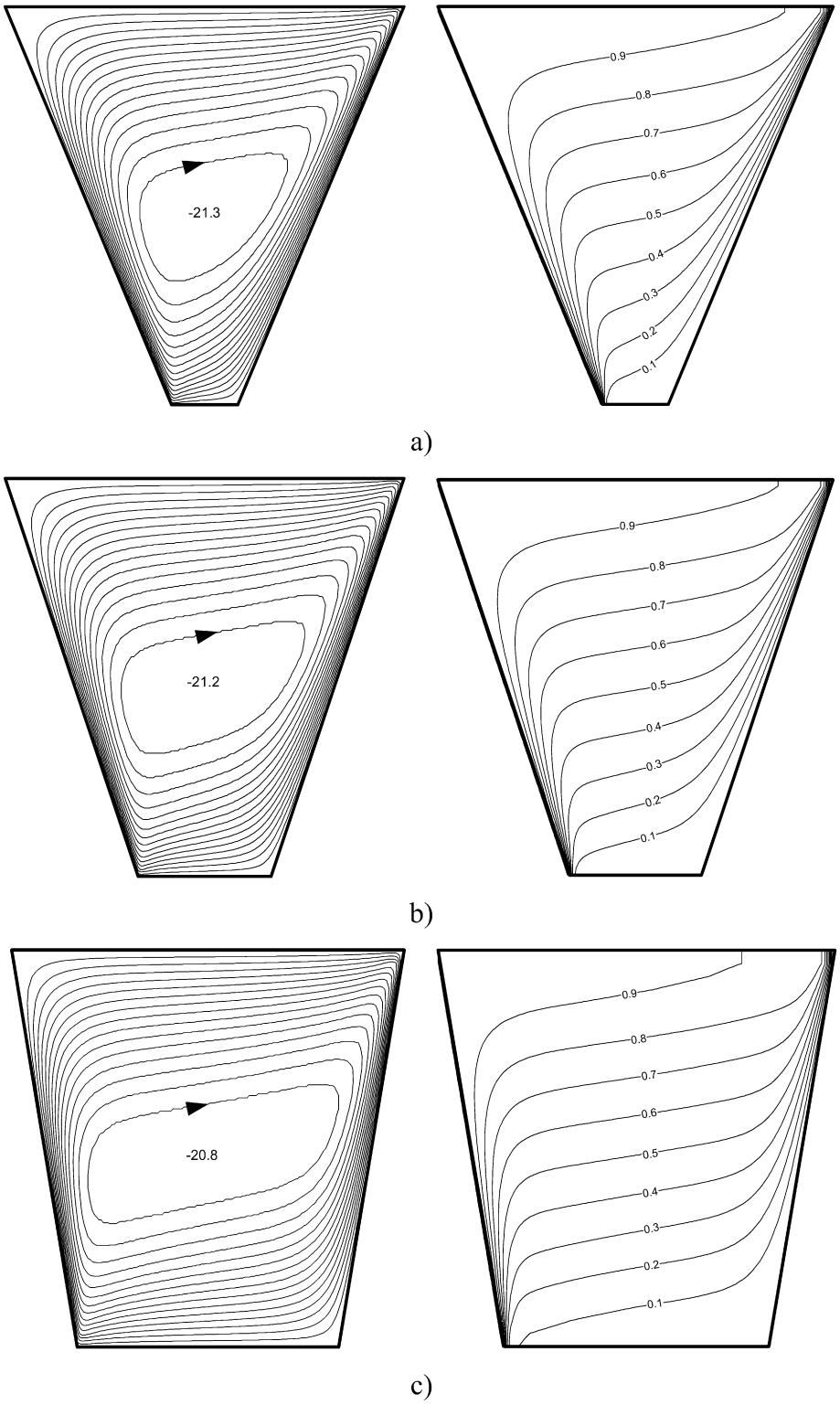

Fig. 3. Streamlines (on the left) and isotherms (on the right) for $A = 1.0$, $Ra = 1000$, $\phi = 0°$; (a) $\theta_s = 67°$, (b) $\theta_s = 72°$, (c) $\theta_s = 81°$.

3. Results and discussion

In this numerical work, there are some governing parameters, which describe different physical behaviour of the flow and heat transfer in natural convection in an inclined porous trapezoidal enclosure, such as orientation or inclination angle ϕ, angle of the sloping wall θ_s, aspect ratio A and Rayleigh number Ra. In the next subsections, we will discuss the effects of these parameters on the flow and heat transfer characteristics.

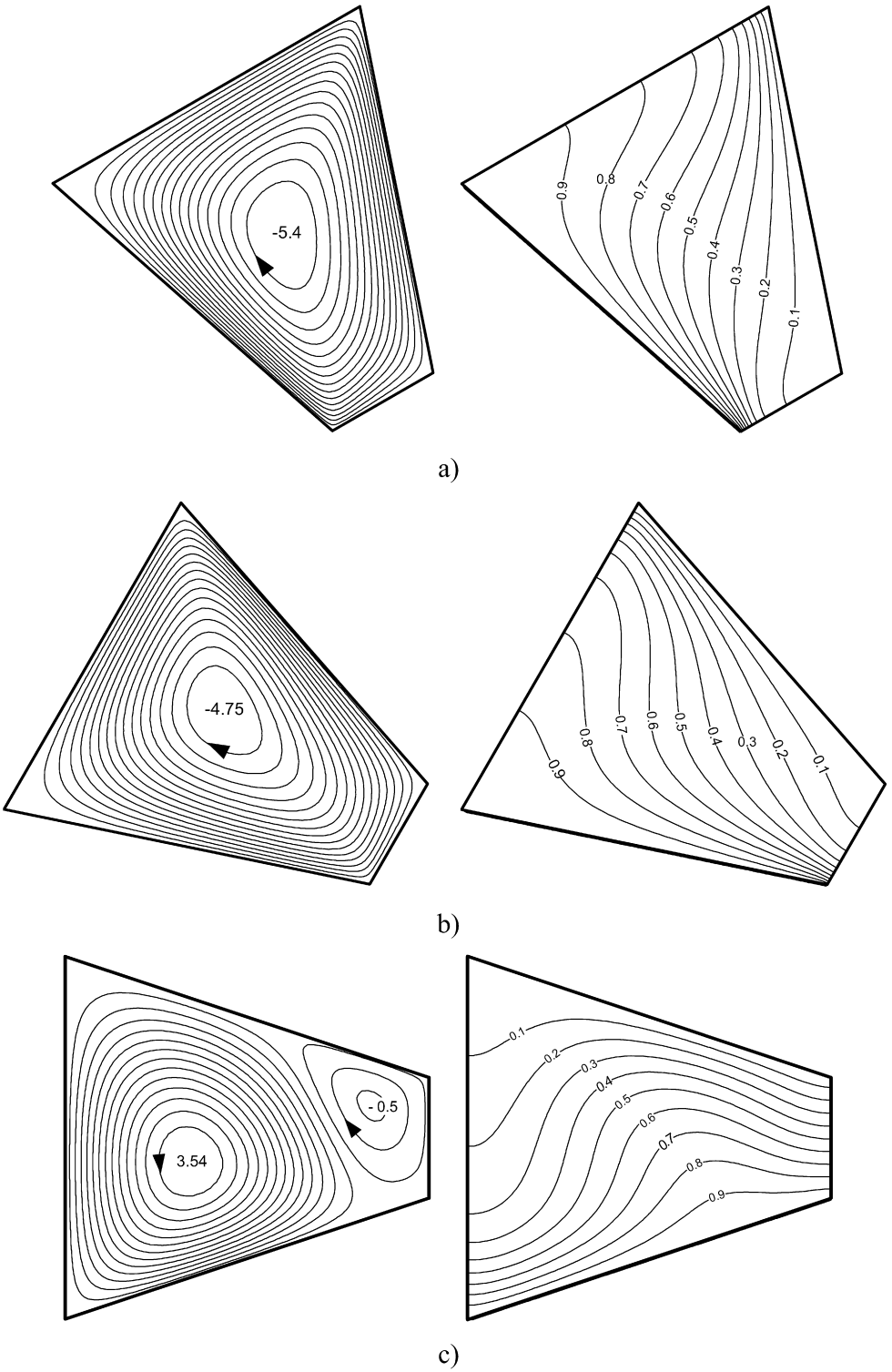

Fig. 4. Streamlines (on the left) and isotherms (on the right) for $A = 1.0$, $Ra = 100$, $\theta_s = 72°$; (a) $\phi = 30°$, (b) $\phi = 60°$, (c) $\phi = 90°$, (d) $\phi = 120°$, (e) $\phi = 150°$, (f) $\phi = 180°$.

3.1. Effects of Rayleigh number

The effects of the Rayleigh numbers *Ra* on the flow field and temperature distribution have been investigated in this subsection. Fig. 2 shows streamlines (on the left) and isotherms (on the right) for different values of *Ra* and for $A = 1.0$, $\theta_s = 72°$ and $\phi = 0°$ (horizontal enclosure). A single rotating cell in clockwise direction is observed inside the enclosure and its strength is increased with increasing *Ra*. This can be seen from absolute values of the minimum stream function. In other words, the flow gets intensified with increasing of *Ra*. This result shows good agreement with the study of Kumar

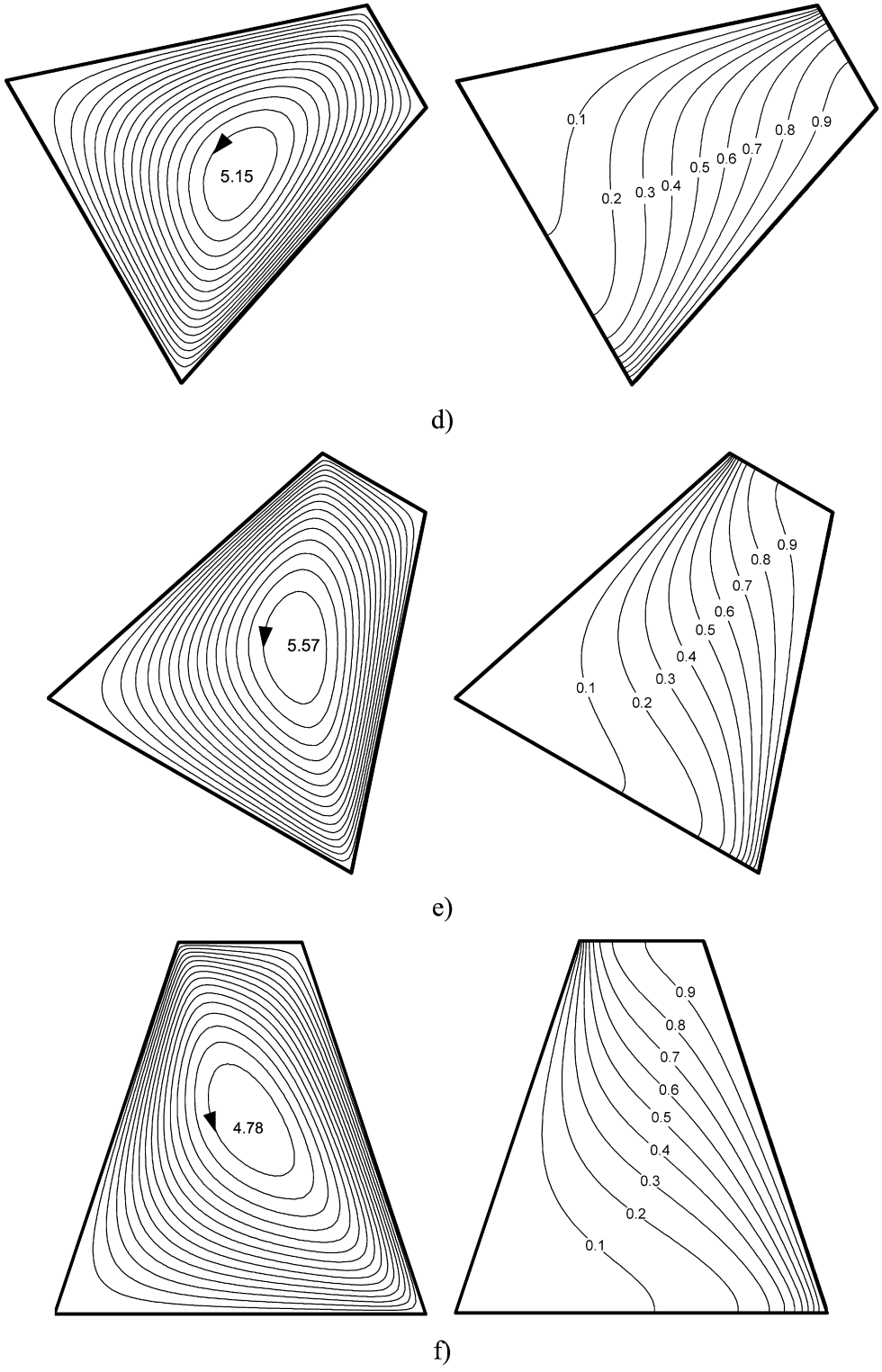

Fig. 4. *(Continued.)*

and Kumar [32] for the same range of the Rayleigh number and position. Isotherms illustrate an almost parallel distribution to the horizontal walls, which indicates the strong conduction. Sharper thermal boundary layer is formed with increasing *Ra*. Further, the effects of the side wall inclination angle θ_s on the temperature and flow fields are presented in Fig. 3 for $A = 1.0$, $Ra = 1000$ and $\phi = 0°$. It is seen that the parameter θ_s does not have any influence on the number of cells or rotating direction of the cells. As can be seen from Figs. 2 and 3, the length of the cells become larger with increasing of volume of the enclosure. However, the strength of flow decreases with increasing the values of the parameter θ_s. The

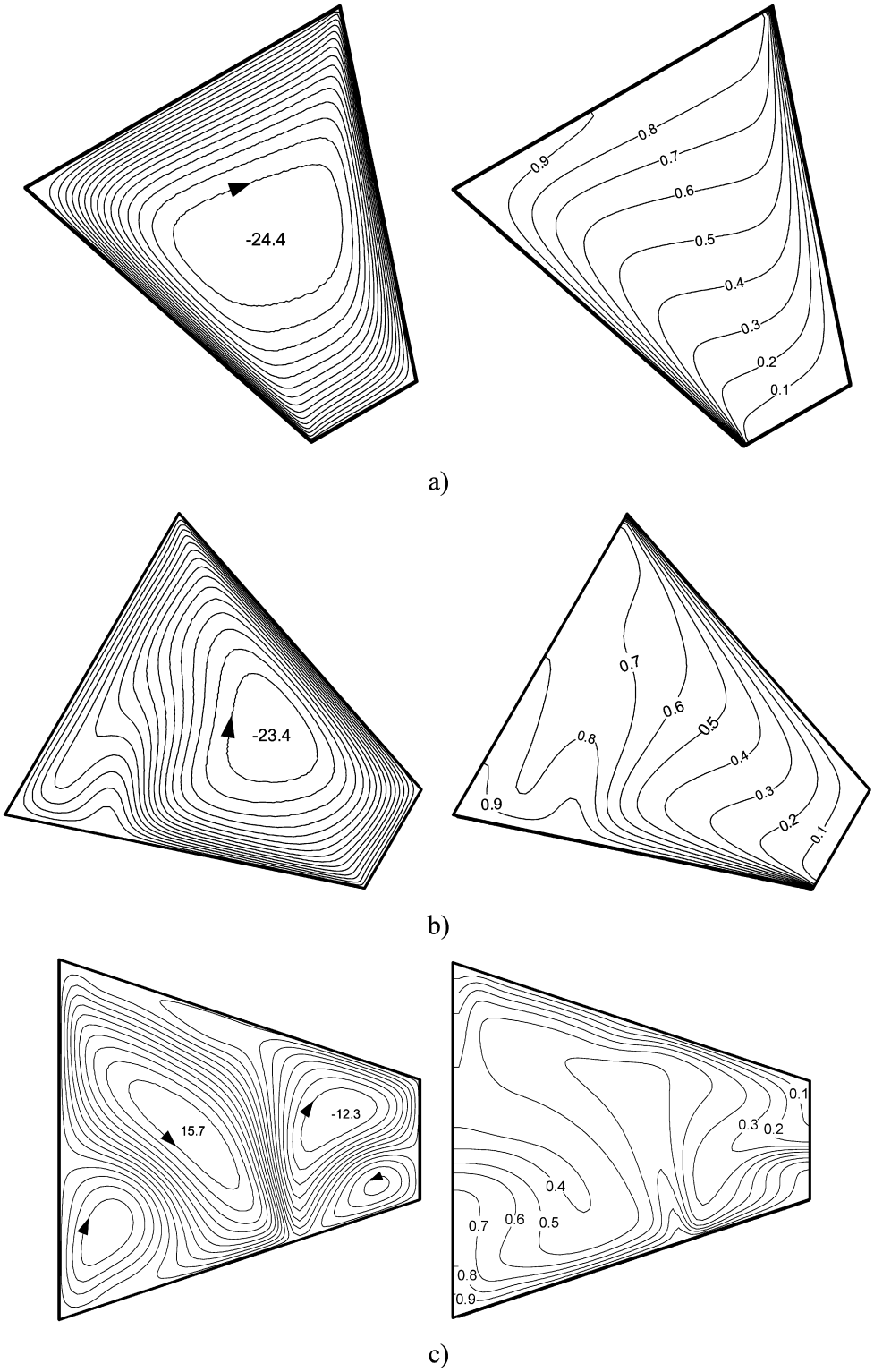

Fig. 5. Streamlines (on the left) and isotherms (on the right) for $A = 1.0$, $Ra = 1000$, $\theta_s = 72°$; (a) $\phi = 30°$, (b) $\phi = 60°$, (c) $\phi = 90°$, (d) $\phi = 120°$, (e) $\phi = 150°$, (f) $\phi = 180°$.

temperature distribution near the boundary is also affected with changing of side wall inclination angle θ_s. Contours are cumulated near the wall for lower value of θ_s. For the highest value of θ_s, results resemble to the benchmark enclosure geometry, see Elsherbiny [19].

3.2. Effects of inclination angles

In this part of the study, the effects of inclination or orientation angle ϕ and side wall inclination angle θ_s are analyzed for different values. Fig. 4 illustrates the effects of ϕ on the

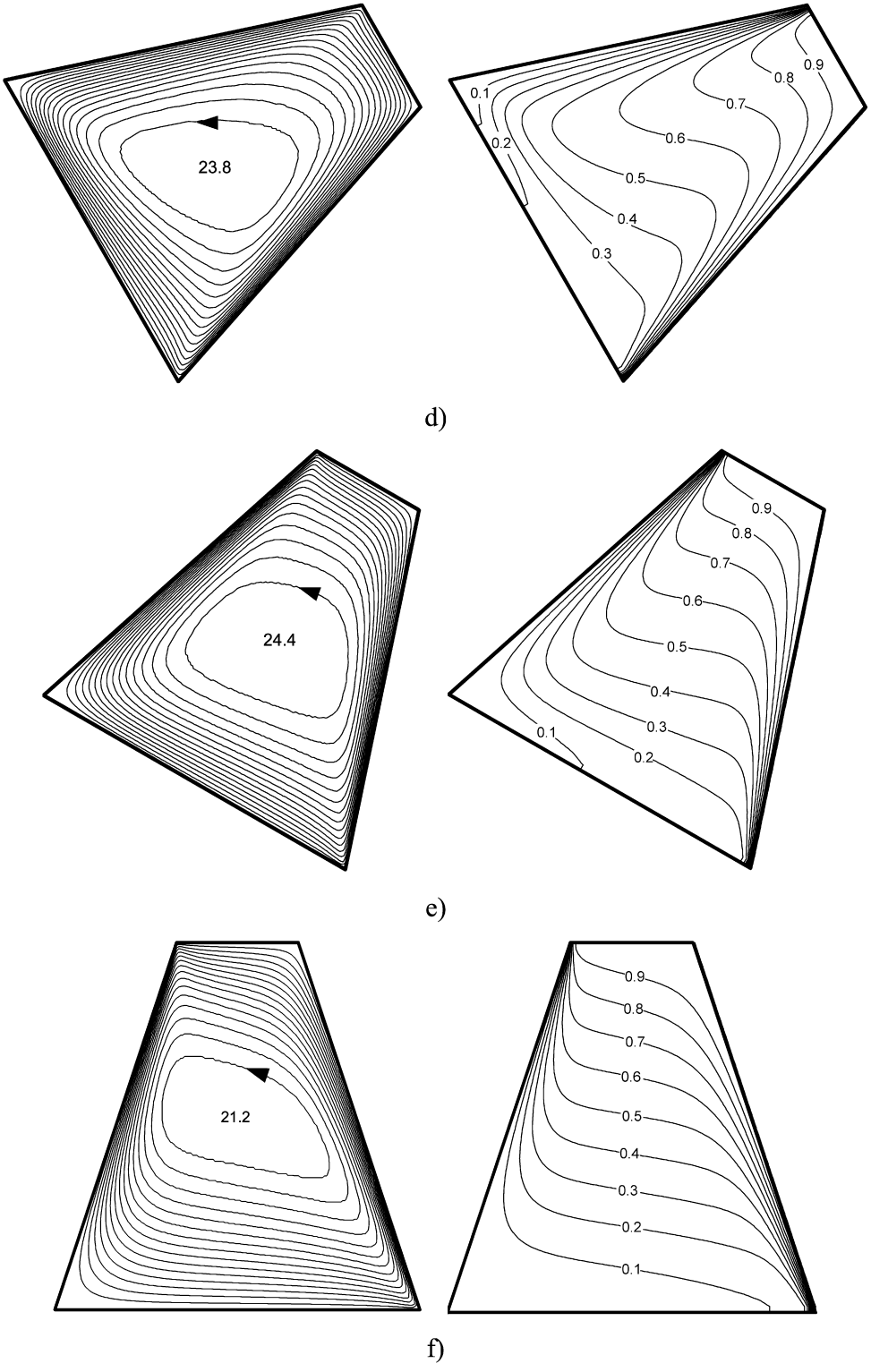

Fig. 5. *(Continued.)*

flow and temperature distributions by plotting streamlines (left) and isotherms (right), respectively. These figures are given for $A = 1.0$, $Ra = 100$ and $\theta_s = 72°$. A single cell in clockwise (CW) direction is formed and its strength increases with increasing the values of ϕ. However, double cells are formed at $\phi = 90°$, which is a critical inclination angle. In this case, the cavity is heated from the sloping bottom wall and cooled from the sloping top wall and the cell, which rotates counterclockwise, is dominant over the clockwise one, due to long heater part of the enclosure. A small cell is located at right top corner of the enclosure. For higher values of ϕ a single cell is again formed but its direction changes from clockwise to coun-

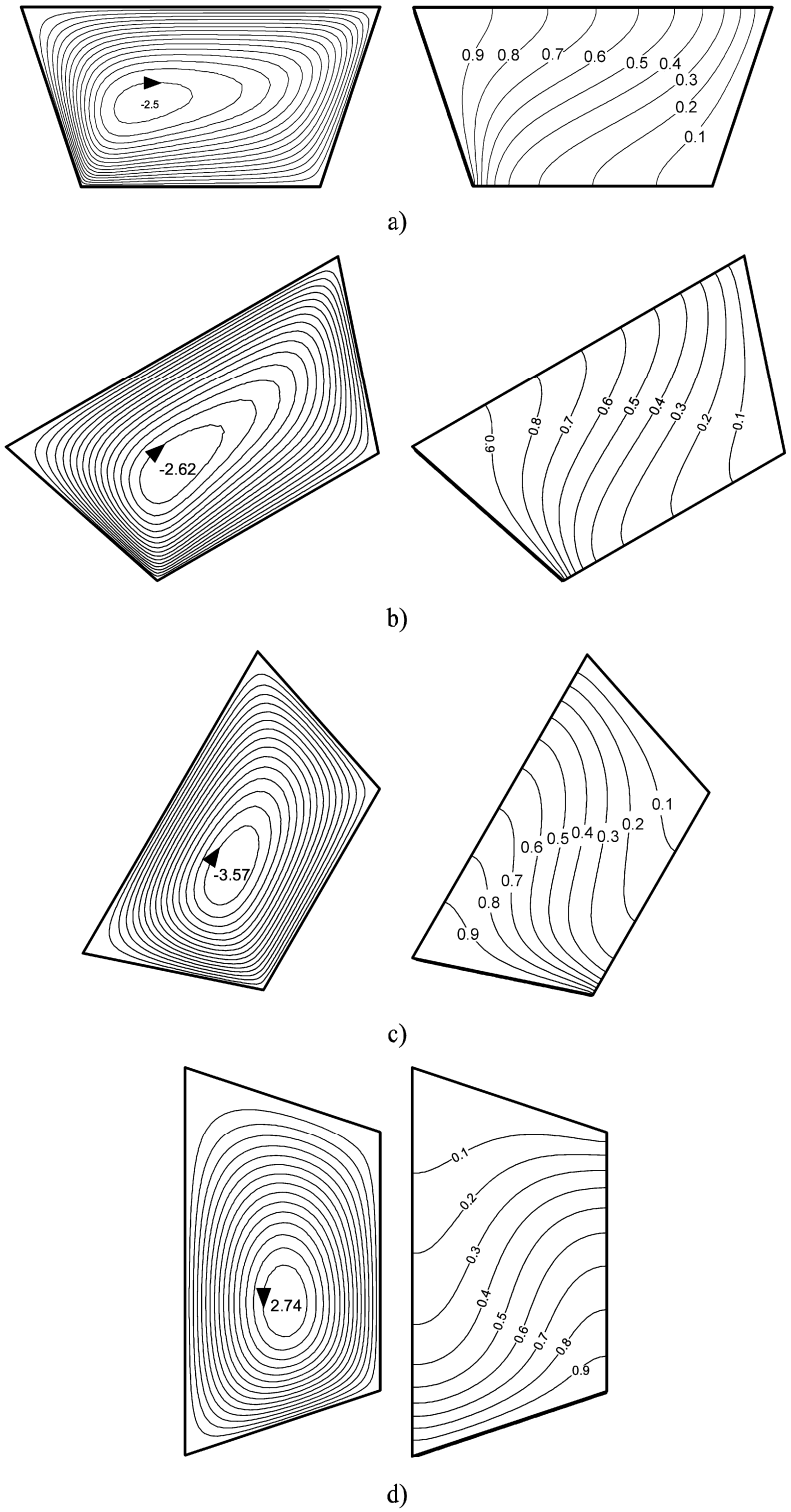

Fig. 6. Streamlines (on the left) and isotherms (on the right) for $A = 0.5$, $Ra = 100$, $\theta_s = 72°$; (a) $\phi = 0°$, (b) $\phi = 30°$, (c) $\phi = 60°$, (d) $\phi = 90°$, (e) $\phi = 120°$, (f) $\phi = 150°$, (g) $\phi = 180°$.

terclockwise, respectively. With increasing of the inclination angle ϕ, the center of the cell moves to the center of trapezoidal enclosure. However, the effects of ϕ on thermal boundary layer is small, except for $\phi = 90°$. For $\phi > 90°$, contrary to Figs. 2 and 3, heat transfer increases at the top region of the trapezoidal enclosure due to short distance between hot and cold walls.

Fig. 5 presents the streamlines (left) and isotherms (right) for different values of ϕ and the same values of the parameters A and θ_s of those in Fig. 4. In this case, the effects of increasing of Ra on the flow and temperature fields can be tested. Both values of the stream function and length of the main cell become larger as Ra increases. A trapezoidal shaped main cell is formed

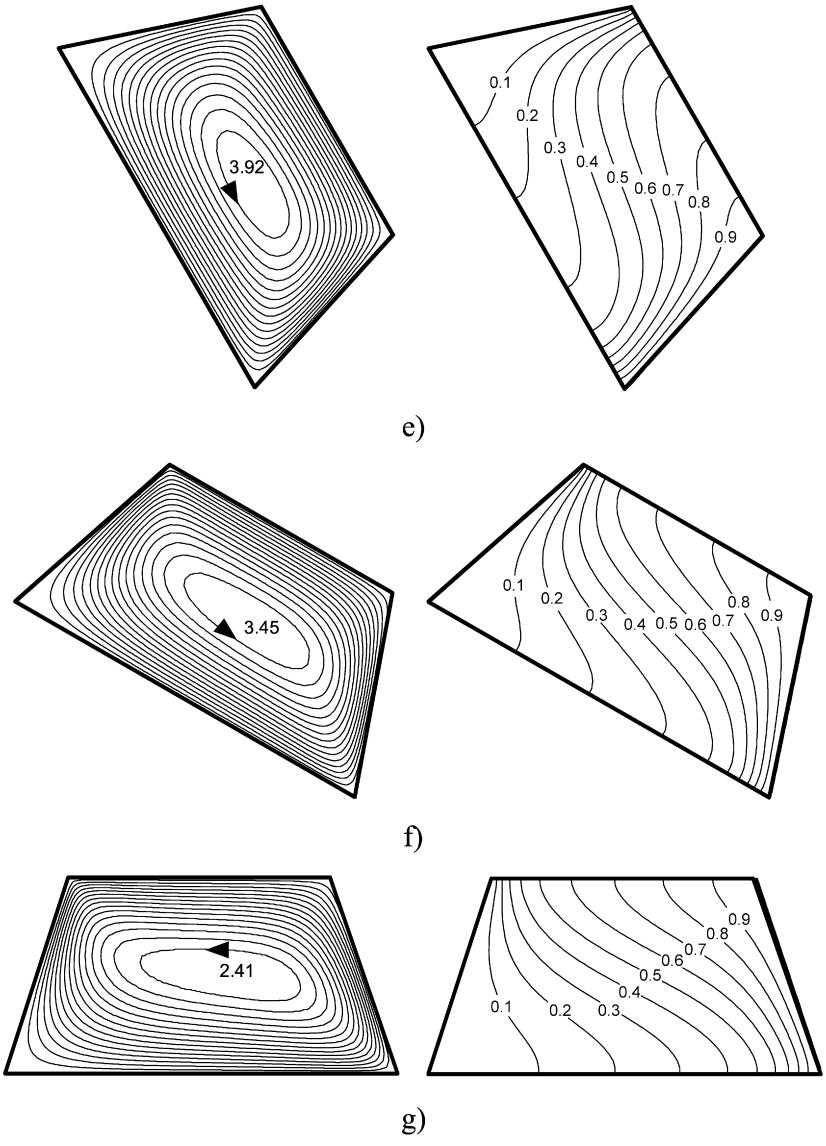

Fig. 6. *(Continued.)*

due to high flow velocity. Distribution of isotherms show sinusoidal shaped variation in the middle of the enclosure but they are parallel to the adiabatic walls, as shown in Fig. 5(a). It can be seen that for higher inclination angle, $\phi = 60^\circ$ say, the main cell moves to the narrow region of the enclosure. In addition, the isotherms show a plume-like distribution at the wide region. However, at $\phi = 90^\circ$ multiple cells are formed due to Bénard cell configuration. For higher values of the inclination angle ϕ, again single cell is formed at counterclockwise direction. Further, Figs. 6 and 7 illustrate the streamlines and isotherms for values of $A = 0.5$ at $Ra = 100$ and $Ra = 1000$, respectively. We have also tested the case of $\phi = 0^\circ$ to search the effects of aspect ratio A on a horizontal ($\phi = 0^\circ$) trapezoidal enclosure (shallow enclosure). In this case, a small single cell has been observed near the left sloping hot wall with $\Psi_{\min} = -2.5$. Its length and absolute values are increased with the increase of inclination angle ϕ. For $\phi = 90^\circ$, the direction of flow circulation changes and the cell rotates in counterclockwise. For higher values of ϕ, the length of cell becomes larger and it sits at the center of enclosure. However, isotherms show regular distribution between hot and cold wall due to slow flow velocity. For the highest values of Ra, namely $Ra = 1000$ say, a long circulation cell is formed and it rotates in clockwise direction. Its length becomes smaller up to $\phi = 90^\circ$. At this value of ϕ, double symmetrical cells are formed. For $\phi > 90^\circ$, the length of circulation cell increases again and it rotates in counterclockwise direction. When the adiabatic walls of the trapezoidal enclosure become parallel to the x-axis, an almost parallel temperature distribution is observed. However, isotherms show wavy variation for other values of the inclination parameter ϕ. It means that both aspect ratio A and the inclination angle ϕ can be used as control parameters for flow and temperature distribution in this problem, especially at high values of the Rayleigh number Ra.

3.3. Heat transfer

Effects of the inclination or orientation angle ϕ on heat transfer are presented for different Rayleigh numbers Ra in Figs. 8(a)

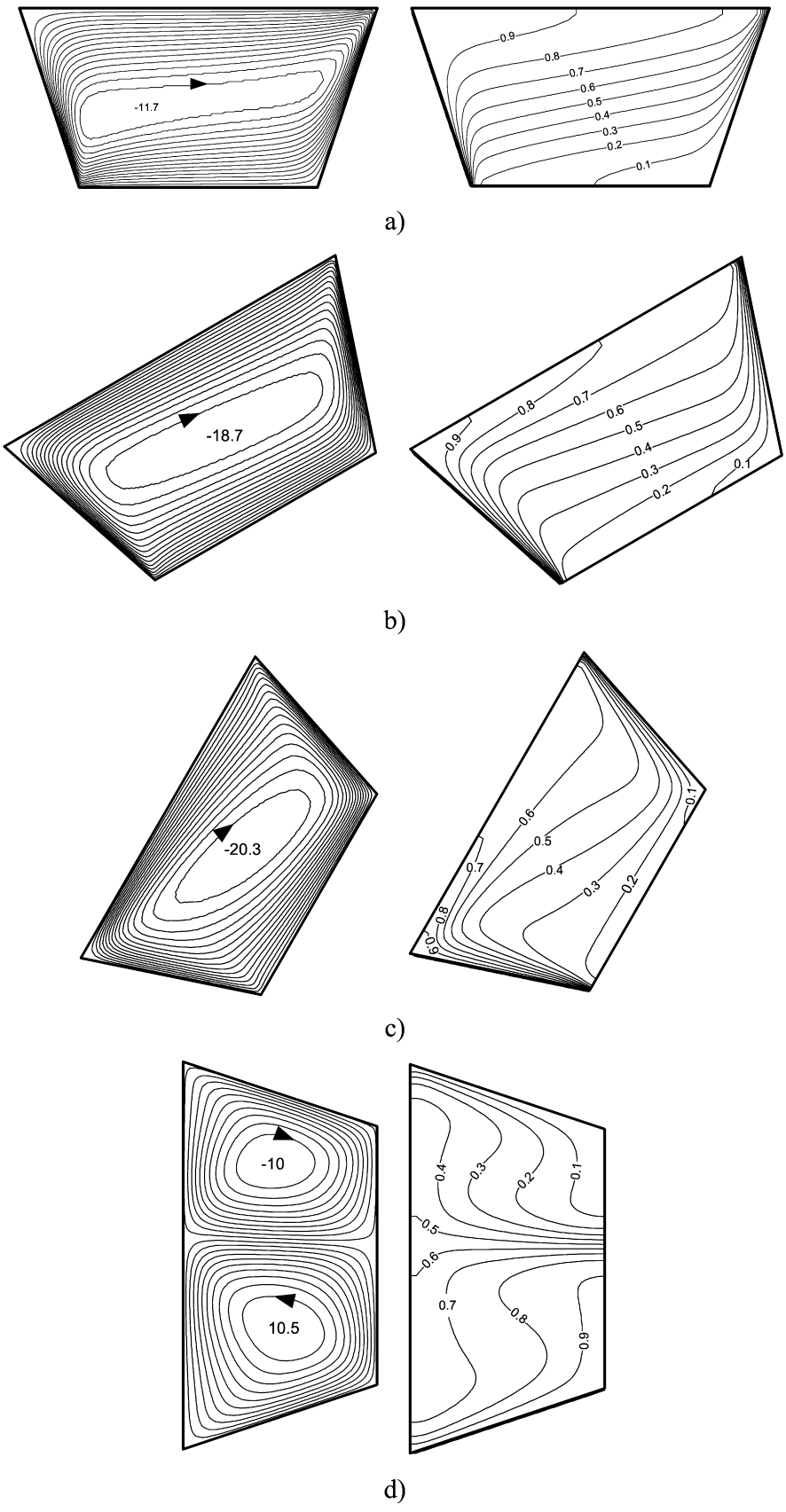

Fig. 7. Streamlines (on the left) and isotherms (on the right) for $A = 0.5$, $Ra = 1000$, $\theta_s = 72°$; (a) $\phi = 0°$, (b) $\phi = 30°$, (c) $\phi = 60°$, (d) $\phi = 90°$, (e) $\phi = 120°$, (f) $\phi = 150°$, (g) $\phi = 180°$.

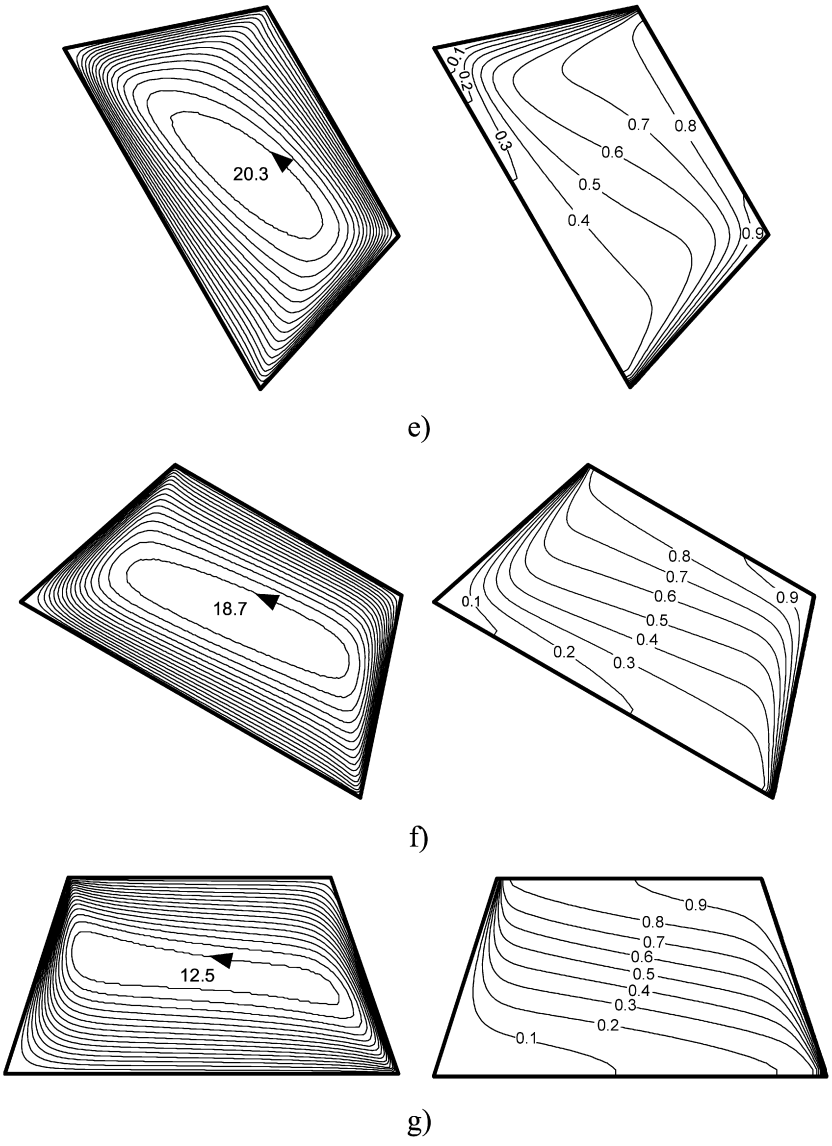

Fig. 7. *(Continued.)*

and (b). The results are presented via the mean Nusselt number Nu_m. For $Ra = 100$, the inclination angle ϕ does not have any influence on Nu_m for both values of the side wall inclination angles considered, $\theta_s = 67°$ (Fig. 8(a)) and $\theta_s = 81°$ (Fig. 8(b)), respectively Thus, there is no Bénard regime for this value of the Rayleigh number. As can be further seen from these figures, Nu_m tends to increase when the cavity is inclined between $\phi = 0°$ and $\phi = 30°$ for higher values of Ra. A minimal value of Nu_m has been observed at $\phi = 90°$. This fact is supported by Baytas's study [40]. The physical mechanism behind this conclusion is that both the convective effect of the hot wall and the unstable effect of the cold wall are reduced by the inclination angle ϕ in accordance with the decrease in buoyancy force due to inclination of the cavity, as indicated by Aydin et al. [17]. The Bénard regime is occurred between $\phi = 70°$ and $\phi = 100°$ for both $\theta_s = 67°$ and $\theta_s = 81°$. But higher values of Nu_m are obtained in the case of $\theta_s = 67°$ inside the range of Bénard regime. But the convection effect becomes more significant for $\phi > 90°$. However, the effect of inclination angle ϕ is more significant for the highest value of Ra due to strong convection mode of heat transfer. Values of Nu_m are almost equal for $\phi = 0°$ and 180° at different values of θ_s.

Fig. 9 shows the variation of the mean Nusselt number Nu_m with the inclination angle ϕ for three values of θ_s when $Ra = 1000$ and $A = 0.5$. The Bénard regime is plotted with dashed lines and other lines at the left and right sides of this region show unicellular flow. As can be seen from this figure, Nu_m has an almost sinusoidal trend between $\phi = 0°$ and 180°. The values of Nu_m decrease with increasing of sidewall inclination angle θ_s and are close to the values for a square enclosure. These values are close to each other up to $\phi = 90°$. As it is illustrated in Fig. 9, the side wall inclination parameter θ_s is also an effective parameter for the onset of Bénard cells for the same values of the parameters Ra and A. Thus, the onset of Bénard regime is for $\phi = 90°$ and $\theta_s = 67°$; $\phi = 85°$ and $\theta_s = 67°$; $\phi = 80°$ and $\theta_s = 72°$. In the range

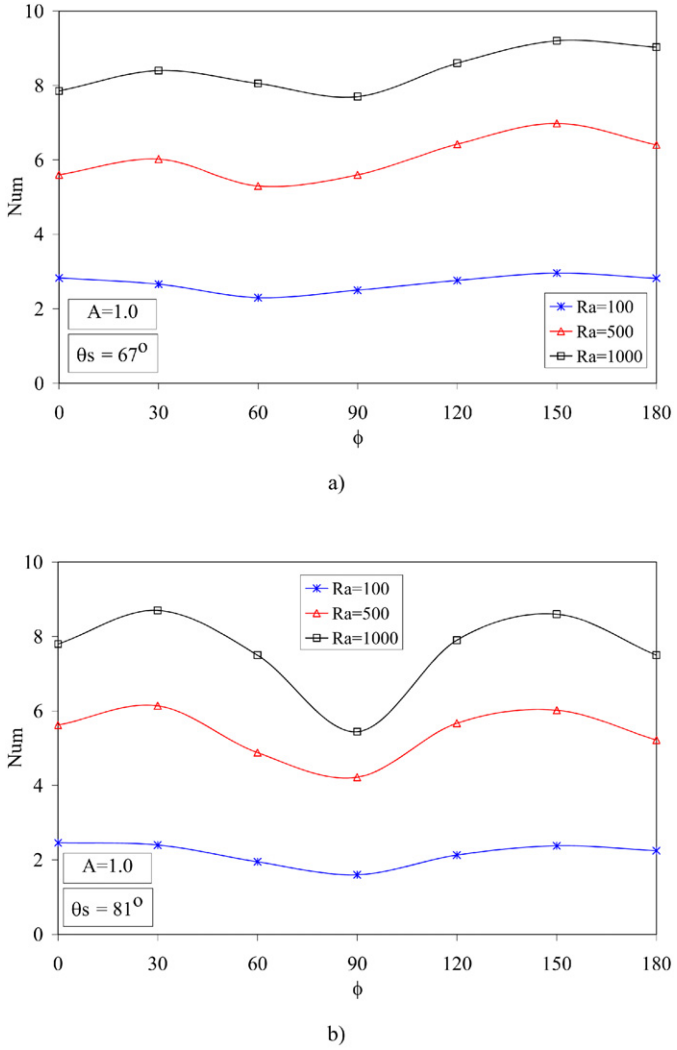

Fig. 8. Variation of the mean Nusselt number with inclination angle for different values of the Rayleigh number when $A = 1.0$: (a) $\theta_s = 67°$, (b) $\theta_s = 81°$.

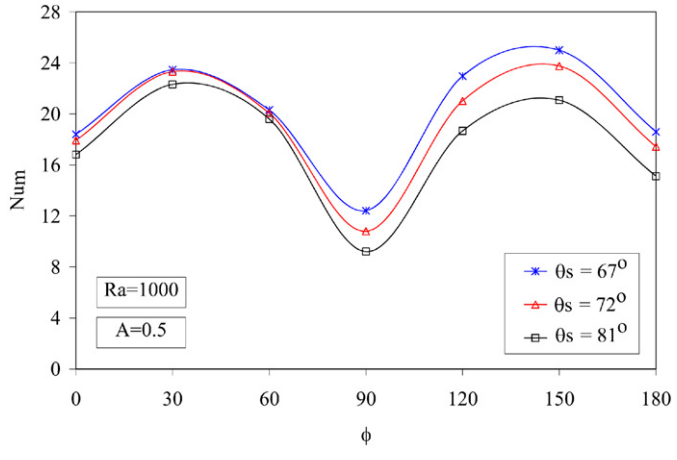

Fig. 9. Variation of the mean Nusselt number with inclination angle for and different values of the inclination side wall angle when $Ra = 1000$, $A = 0.5$.

$90° \leqslant \phi \leqslant 180°$, a substantial difference was observed for Nu_m with the increasing of convection mode of heat transfer.

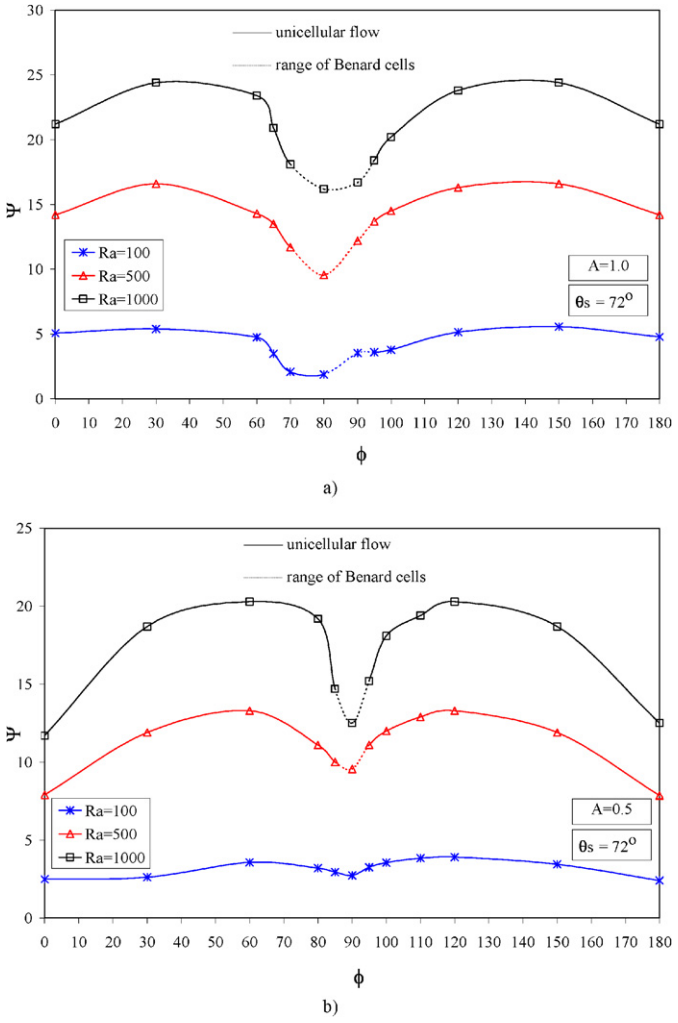

Fig. 10. Variation of the extremum values of stream function with inclination angle for different Rayleigh numbers when $\theta_s = 72°$; (a) $A = 1.0$, (b) $A = 0.5$.

3.4. *Effects of aspect ratio*

Variation of the flow strength is presented in Figs. 10(a) and (b) via values of the absolute extremum stream function for $\theta_s = 72°$ and different values of the inclination angles ϕ. An analysis has been also performed for different values of the aspect ratio A of the enclosure. Similar trends were observed between values of the absolute extremum of the stream function and the mean Nusselt number Nu_m. It means that both heat transfer and fluid flow are affected at the same magnitude by the governing parameters ϕ and A. The values of the stream function increase slightly for values of the inclination parameter ϕ between 0° and 60°. The Bénard regime is also observed for $Ra = 100$ and values of ϕ in the range $80° \leqslant \phi \leqslant 95°$. However, the changes of Bénard cells depend also by Ra. For a highest value of the Rayleigh number, $Ra = 1000$ say, the Bénard cells change for values of ϕ in the range $70° \leqslant \phi \leqslant 95°$. A minimum is reached at $\phi = 90°$ due to low fluid velocity. The inclination angle ϕ is, therefore, an important parameter on the flow strength for higher values of Ra. When Figs. 10(a) and (b) are compared to see the effect of the parameter A on the flow

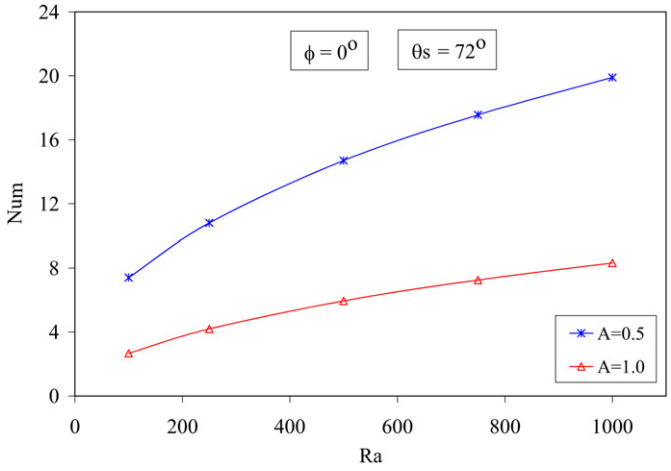

Fig. 11. Variation of mean Nusselt number with different Rayleigh numbers for different aspect ratio when $\phi = 0^\circ$ and $\theta_s = 72^\circ$.

strength, it is observed that the variation of flow strength depends substantially by the values of *Ra*. Finally, Fig. 11 shows the variation of Nu_m with the aspect ratio A. It is seen that the variation of the parameter A is more effective for higher values of *Ra*. Therefore, it can be concluded that both inclination angle ϕ and aspect ratio A can be used to control the flow field and heat transfer inside the porous trapezoidal enclosure.

4. Conclusions

Flow field and heat transfer characteristics have been numerically investigated in this paper for natural convection in an inclined trapezoidal enclosure filled with a fluid-saturated porous medium at different values of inclination angle, sloping wall angle, Rayleigh number and aspect ratio. Based on the obtained results, the findings can be listed as follows:

(1) Overall heat transfer is increased with increasing of the Rayleigh number *Ra* and decreases with decreasing of sloping angle ϕ. For the highest value of the aspect ratio A, the flow becomes stagnant far from the heated wall. The effects of the parameter A on heat transfer depends on the values of *Ra*. However, higher values of *Ra* are more significant on the flow and heat transfer characteristics.
(2) Both the inclination or orientation angle ϕ and the sloping wall angle θ_s affect the temperature distribution and flow field. But the parameter ϕ is a dominant parameter in this problem. It causes a multicellular flow and a minimum heat transfer is obtained at $\phi = 90^\circ$. The sloping wall angle θ_s is more effective for higher values of ϕ.
(3) There can be an optimum solution containing all parameters but this is outside the scope of the present paper. However, the study can be extended to an instability analysis in the future.
(4) The onset of Bénard cells is also affected by the change of both inclination angle of the side wall and the inclination or orientation of the cavity. The Rayleigh number is also an effective parameter for the change of the Bénard regime.

References

[1] D.B. Ingham, I. Pop (Eds.), Transport Phenomena in Porous Media, vol. III, Elsevier, Oxford, 2005.
[2] D.A. Nield, A. Bejan, Convection in Porous Media, third ed., Springer, New York, 2006.
[3] D.B. Ingham, A. Bejan, E. Mamut, I. Pop, Emerging Technologies and Techniques in Porous Media, Kluwer, Dordrecht, 2004.
[4] A. Bejan, I. Dincer, S. Lorente, A.F. Miguel, A.H. Reis, Porous and Complex Flow Structures in Modern Technologies, Springer, New York, 2004.
[5] K. Vafai (Ed.), Handbook of Porous Media, second ed., Taylor & Francis, New York, 2005.
[6] K.L. Walker, G.M. Homsy, Convection in porous cavity, J. Fluid Mech. 87 (1978) 449–474.
[7] A. Bejan, On the boundary layer regime in a vertical enclosure filled with a porous medium, Lett. Heat Mass Transfer 6 (1979) 93–102.
[8] V. Prasad, F.A. Kulacki, Convective heat transfer in a rectangular cavity-effect of aspect ratio on flow structure and heat transfer, J. Heat Transfer 106 (1984) 158–165.
[9] C. Beckermann, R. Viskanta, S. Ramadhyani, A numerical study of non-Darcian natural convection in a vertical enclosure filled with a porous medium, Numer. Heat Transfer 10 (1986) 557–570.
[10] R.J. Gross, M.R. Bear, C.E. Hickox, The application of flux-corrected transport (FCT) to high Rayleigh number natural convection in a porous medium, in: Proc. Eighth Int. Heat Transfer Conf., San Francisco, CA, 1986.
[11] F.C. Lai, F.A. Kulacki, Natural convection across a vertical layered porous cavity, Int. J. Heat Mass Transfer 31 (1988) 1247–1260.
[12] B. Goyeau, J.P. Songbe, D. Gobin, Numerical study of double-diffusive natural convection in a porous cavity using the Darcy–Brinkman formulation, Int. J. Heat Mass Transfer 39 (1996) 1363–1378.
[13] D.M. Manole, J.L. Lage, Numerical benchmark results for natural convection in a porous medium cavity, in: Heat and Mass Transfer in Porous Media, ASME Conference, HTD-vol. 216, 1992, pp. 55–60.
[14] E. Choi, A. Chamkha, K. Nandakumar, A bifurcation study of natural convection in porous media with internal heat sources: the non-Darcy effects, Int. J. Heat Mass Transfer 41 (1998) 383–392.
[15] M. Mamou, P. Vasseur, E. Bilgen, Double-diffusive convection instability in a vertical porous enclosure, J. Fluid Mech. 368 (1998) 263–289.
[16] N.H. Saeid, I. Pop, Natural convection from a discrete heater in a square cavity filled with a porous medium, J. Porous Media 8 (2005) 55–63.
[17] O. Aydin, A. Unal, T. Ayhan, A numerical study on buoyancy-driven flow in an inclined square enclosure heated and cooled on adjacent walls, Numer. Heat Transfer Part A 36 (1999) 585–599.
[18] M.C. Ece, E. Buyuk, Natural-convection flow under a magnetic field in an inclined rectangular enclosure heated and cooled on adjacent walls, Fluid Dynam. Res. 38 (2006) 564–590.
[19] S.M. Elsherbiny, Free convection in inclined air layers heated from above, Int. J. Heat Mass Transfer 39 (1996) 3925–3930.
[20] H.F. Oztop, Natural convection in partially cooled and inclined porous rectangular enclosures, Int. J. Thermal Sci. 46 (2007) 149–156.
[21] R.A. Kuyper, Th.H. Van Der Meer, C.J. Hoogendoorn, R.A.W.M. Henkes, Numerical study of laminar and turbulent natural convection in an inclined square cavity, Int. J. Heat Mass Transfer 36 (1993) 2899–2911.
[22] M. Rahman, M.A.R. Sharif, Numerical study of laminar natural convection in inclined rectangular enclosures of various aspect ratios, Numer. Heat Transfer Part A 44 (2003) 355–373.
[23] P. Vasseur, M.G. Satish, L. Robillard, Natural convection in a thin, inclined, porous layer exposed to a constant heat flux, Int. J. Heat Mass Transfer 30 (1987) 537–549.
[24] A.C. Baytas, Entropy generation for natural convection in an inclined porous cavity, Int. J. Heat Mass Transfer 43 (2000) 2089–2099.
[25] S.L. Moya, E. Ramos, M. Sen, Numerical study of natural convection in a tilted rectangular porous material, Int. J. Heat Mass Transfer 30 (1987) 741–756.
[26] D. Poulikakos, A. Bejan, Numerical study of transient high Rayleigh number convection in an attic-shaped porous layer, J. Heat Transfer 105 (1983) 476–484.

[27] Y. Varol, H.F. Oztop, A. Varol, Natural convection in porous triangular enclosures with a solid adiabatic fin attached to the horizontal wall, Int. Comm. Heat Mass Transfer 34 (2007) 19–27.
[28] A. Bejan, D. Poulikakos, Natural convection in an attic-shaped space filled with porous material, J. Heat Transfer 104 (1982) 241–246.
[29] Y. Varol, H.F. Oztop, T. Yilmaz, Two-dimensional natural convection in a porous triangular enclosure with a square body, Int. Comm. Heat Mass Transfer 34 (2007) 238–247.
[30] Y. Varol, H.F. Oztop, A. Varol, Effects of thin fin on natural convection in porous triangular enclosures, Int. J. Thermal Sci. 46 (2007) 1033–1045.
[31] A.C. Baytas, I. Pop, Free convection in oblique enclosures filled with a porous medium, Int. J. Heat Mass Transfer 42 (1999) 1047–1057.
[32] B.V.R. Kumar, B. Kumar, Parallel computation of natural convection in trapezoidal porous enclosures, Math. Comput. Simulation 65 (2004) 221–229.
[33] A.C. Baytas, I. Pop, Natural convection in a trapezoidal enclosure filled with a porous medium, Int. J. Eng. Sci. 39 (2001) 125–134.
[34] T.S. Lee, Numerical experiments with fluid convection in tilted nonrectangular enclosures, Numer. Heat Transfer Part A 19 (1991) 487–499.
[35] M. Boussiad, A. Mezenner, M. Bouhadel, Convection naturelle de chaleur et de masse dans une cavite trapezoidale, Int. J. Thermal Sci. 38 (1999) 363–371.
[36] J.T. Van Der Eyden, T.H. Van Der Meer, K. Hanjalic, E. Biezen, J. Bruining, Double-diffusive natural convection in trapezoidal enclosures, Int. J. Heat Mass Transfer 41 (1998) 1885–1898.
[37] S. Kumar, Natural convective heat transfer in trapezoidal enclosure of box-type solar cooker, Renewable Energy 29 (2004) 211–222.
[38] E. Papanicolaou, V. Belessiotis, Double-diffusive natural convection in an asymmetric trapezoidal enclosure: unsteady behavior in the laminar and the turbulent-flow regime, Int. J. Heat Mass Transfer 48 (2005) 191–209.
[39] M. Boussaid, A. Djerrada, M. Bouhadef, Thermosolutal transfer within trapezoidal cavity, Numer. Heat Transfer Part A 43 (2003) 431–448.
[40] A.C. Baytas, Entropy generation for natural convection in an inclined porous cavity, Int. J. Heat Mass Transfer 43 (2000) 2089–2099.